Modeling and Analysis on Position and Gesture of End-Effector of Cleaning Robot Based on Monorail Bogie for Solar Panels

Chengwei Shen[1], Lubin Hang[1(✉)], Jun Wang[1], Wei Qin[1], Yabo Huangfu[1], Xiaobo Huang[1], and Yan Wang[2]

[1] Shanghai University of Engineering Science, Shanghai 201620, China
hanglb@126.com
[2] Shanghai Jiaotong University, Shanghai 200240, China

Abstract. The dust particles on solar panel surface have a serious influence on the consistency and efficiency of photovoltaic power station, a new cleaning robot based on monorail bogie technology using for automatic cleaning of solar panel is presented in this paper. Position and gesture of the end-effector are critical to the quality and efficiency of work. According to the mechanical structure and motion mechanism of the bogie, five hypotheses which simplify the robot-rails system as a double masses-spring-damper model are proposed. The governing motion equations of the robot during travel process are established, and then the corresponding position and gesture of end-effector within motion range are determined by analyzing dynamics responses of bogie under the input of end-effector's motion. The simulation model under this defined function is built and curves of position and gesture are plotted based on Simulink. A prototype is fabricated and tested by Leica laser tracker, which shows that the position and gesture of the end-effector are related to its working position.

Keywords: Cleaning robot for solar panel · Monorail bogie technology · End-effector · Robot-rails system · Dynamics responses · Position and gesture

1 Introduction

Environment conflict appears particularly prominent along with mineral resource's gradual depletion. As a renewable sources of energy, solar power has been attached more and more importance. Solar industry, which has become one of tendencies in the field of new energy industry, is developing fast in many countries [1]. Solar panel is the core component of the solar power generation system and its photoelectricity conversion efficiency will affect the performance of system directly. At present, research on photoelectricity conversion efficiency of solar panel has concentrated on power generation technology [2] and application of materials [3].

Yet dust particles, in the air, on solar panel also reduce photoelectricity conversion efficiency [4], especially in the large system of PV power station. Under these circumstances, it is necessary to clean solar panel while vibration of panels and generation of water spots should be avoided during cleaning process. Automated cleaning system

N. Kubota et al. (Eds.): ICIRA 2016, Part I, LNAI 9834, pp. 122–133, 2016.
DOI: 10.1007/978-3-319-43506-0_11

of the large photovoltaic array has not yet universal by far, so mechanical design and research on clean of solar panel has great value in application.

For cleaning of large panels and special equipment, robot "Sky wash" [5], carried by vehicle chassis, cleans different types of plane via a multi-joint manipulator, which is used by Lufthansa Flight. Cleanbot-III, designed by City University of Hong Kong, can crawl over the panel and cross the barrier via a chassis composed of vacuum-absorb machines [6]. Fraunhofer Institute for Production Technology composed cleaning technology with rail engineering technology [7] and developed auto-cleaning system SFR I, this machine can do cleaning work while moving guide track, as shown in Fig. 1. In China, Guan [8] designed a solar panel cleaning machine and optimized the structure of manipulator aiming at cleaning problems of solar panel. Ecoppia, an Israeli company that sets out to robotic solar cleaning solution, developed the robot "ECOPPIA E4" in 2014 [9]. This robot combines a powerful, soft microfiber cleaning system with controlled airflow, as is shown in Fig. 2. E4 leverages Eco-Hybrid technology to recover energy when the robot descends the solar panel, and later reuse this energy to optimize performance.

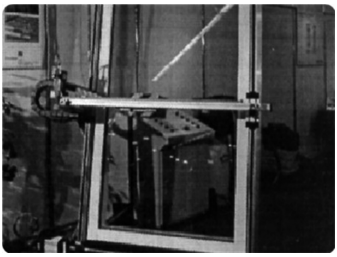

Fig. 1. Auto-cleaning system SFR I

Fig. 2. ECOPPIA E4

In this paper, a robot using flexible bracket of wheels for cleaning solar panel is designed, which can move along the rails of panel support and clean the panel one by one. Quality and efficiency of work can be guaranteed and not affected by potholes on the ground. However, this flexible bracket will affect the position and gesture of robot, under these circumstances, the robot-rails system is simplified as a planar double masses-spring-damper model based on five relative hypothesis and the motion equations of robot during walking status are established. The dynamics responses of the bogie, under the input of end-effector's motion, are analyzed. Then the corresponding position and gesture of end-effector within motion range are determined. A prototype is fabricated, then tested by Leica laser tracker, some conclusions are drawn.

2 Mechanism of Cleaning Robot

The robot using rail-tracked mechanism can guarantee reliability even under poor working conditions. Monorail vehicle has the character of adapting to complex land structure and it becomes the most popular transportation in mountain cities, as shown in

Fig. 3. The monorail bogie, different from wheeled locomotion mechanism in structure [10], moves on the track beam via a pair of running wheels with steering wheels and stabilizing wheels located on the bottom of vehicle body moving on the two sideways of track, as shown in Fig. 4. This ensures the safe and stable operation of vehicle and no risk of running out of the track.

Fig. 3. Monorail transportation

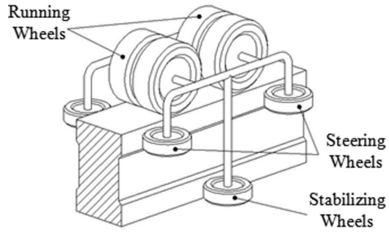

Fig. 4. Structure of monorail bogie

The cleaning robot for running on the solar panel support, which can be seen in Fig. 5, consists of groups of wheels, bogie

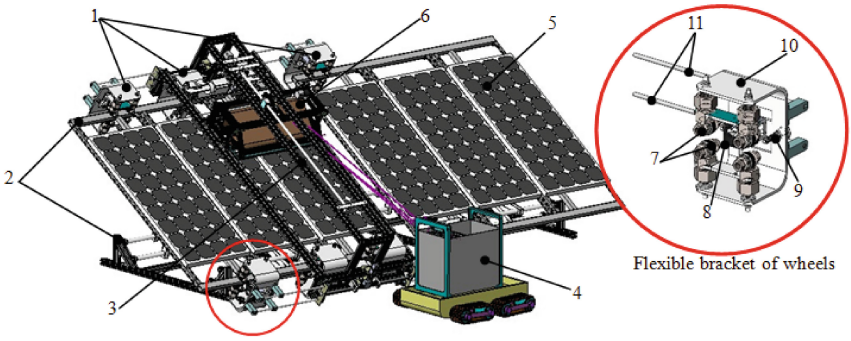

1-Group of wheels 2-Panel support 3-Bogie 4-Water recycle system 5-Solar panel 6-End-effector 7-Clamping wheels 8-Running wheel 9-Springs 10-Bracket 11-Rods

Fig. 5. Assembly of cleaning robot (Color figure online)

and end-effector.

The end-effector is the cleaning device of robot. The movable water tank can supply the end-effector with cleaning liquid and a trio of solar panels is fixed on the panel support. Running wheel and clamping wheels are fitted on the bracket using flexible structure. The close-up which is marked with red circle is shown in Fig. 5. Under work condition, the two-sides clamping wheels contact reliably with metal rails of panel support to guarantee that robot can move directly with running wheels. When the interval of two panel supports is detected, double groups of wheels in front can be

stuck out by the extensive rods to stride over the interval. The end-effector, driven by screw which is located on the bogie, reciprocates on the linear guide of bogie according to working requirements and cleans the surface of solar panel.

To realize the optimum performance of the cleaning robot, the horizontal of bogie need to keep parallel to the surface of solar panel approximately. The solar panel to be cleaned is large and travel range of end-effector is long, so the size of load carried by each wheel of bogie will vary with movement of end-effector while tires' contact with metal rail is guaranteed by the spring between each wheel and bogie, which has inevitable consequences for the position and gesture of bogie, and these of end-effector will also be affected. Therefore, these positions and gestures should be analyzed.

3 Kinematic Model of Cleaning Robot

In the field of robot control, parallel manipulators analysis and vehicle dynamics, mechanical system is simplified as a multi-body connected with spring and damper [11] to analyze its characteristic based on spring-damper unit [12]. Position and gesture of end-effector are closely related to its working condition and structural parameters of robot. The robot-rails system is simplified as a mass-spring-damper model and equations of motion for cleaning robot are established to analyze the motion of bogie, then the corresponding position and gesture of end-effector are determined.

3.1 Model Simplification

The cleaning robot for solar panel is a complex mechanical system, five hypotheses are proposed to simplify model as following.

(1) Bogie, screw and linear guide are described as a mass, and masses of wheels are negligible.
(2) End-effector is simplified as a mass, moves on the bogie, and frictional resistance is negligible.
(3) Each wheel contacts with rails all the time, and no slippage of tire happens.
(4) Yaw angle of bogie is small.

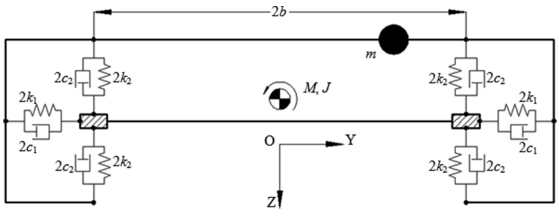

Fig. 6. Robot-rails system

(5) Horizontal and vertical movements of bogie are decoupled [13].

The angle, between panel of most PV power station and ground, is small so the panels can be considered parallel to the ground. During working process of the cleaning robot, the bogie travels at a smooth and low speed. Bogie and rails of panel supports remain relatively constant and static without considering that bogie strides over the interval of panel supports. Ignoring the tire dynamics performance [14], the wheel contacts with rails by the spring, this can be described as a point contact. Then the connection between the point and bogie is represented by a spring-damper unit [15], which is a linear conceptual model. Based on the five hypotheses above, the robot-rails system is simplified as a planar double masses-spring-damper model, as shown in Fig. 6.

In this model, the bogie has three freedoms of translation along Y, translation along Z and rotation about X and the end-effector has only one freedom of translation Y on the linear guide of bogie. M is mass of bogie, J is rotary inertia of bogie about its center of mass, m is mass of end-effector, $2b$ is length of linear guide, k_1 is equivalent stiffness of running wheel, c_1 is equivalent damping of running wheel, k_2 is equivalent stiffness of clamp wheel, c_2 is equivalent damping of running wheel. Furthermore, motion of end-effector on the bogie is the main factor affecting position and gesture of bogie. The corresponding position and gesture of end-effector can be determined by calculating dynamics responses of bogie under the input of end-effector's motion based on the equations of motion for robot.

3.2 Equations of Motion for Robot

Relative displacement of end-effector to bogie can be expressed as

$$y_m - y = S(t) \tag{1}$$

Where $S(t)$ can be described as the motion excitation of the robot-rails system.

According to Newton's laws of motion, the differential equations of motion for robot can be determined as follows.

Horizontal Motion of Robot

As shown in Fig. 7, the static equilibrium position is chosen to be the initial position. By letting y be the displacement of M, y_m be the displacement of m from the static equilibrium, then

$$M\ddot{y} + m\ddot{y}_m = f_{1L} + f_{1R} \tag{2}$$

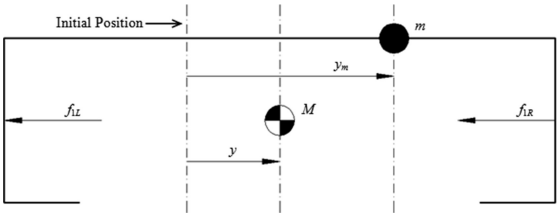

Fig. 7. Robot model under horizontal force

Where f_{1L} and f_{1R} are the horizontal equivalent spring-damper force carried by bogie, and

$$f_{1L} = f_{1R} = -2c_1\dot{y} - 2k_1 y \tag{3}$$

Substituting Eq. (1) into Eq. (2), then Eq. (2) can be written as

$$(M+m)\ddot{y} + 4c_1\dot{y} + 4k_1 y = -m\ddot{S}(t) \tag{4}$$

According to Duhamel's principle [16], the response of the system for the zero initial condition is

$$y(t) = \frac{1}{(M+m)\omega_{d1}} \int_0^t \left(-m\ddot{S}(t)\right) \mathrm{e}^{-\zeta_1 \omega_{n1}(t-\tau)} \sin \omega_{d1}(t-\tau) d\tau \tag{5}$$

Where $\omega_{n1} = \sqrt{\frac{4k_1}{M+m}}$, $\zeta_1 = \frac{4c_1}{2(M+m)\omega_{n1}}$ and $\omega_{d1} = \sqrt{1-\zeta_1^2}\omega_{n1}$.

Vertical Motion of Robot

As shown in Fig. 8, the position that the robot statically contacts the rails of panel support is chosen to be the initial position. By letting z be the displacement and φ be the rotation of bogie from the initial position. $sin\varphi \approx \varphi$ and $cos\varphi \approx 1$ due to the small yaw angle of bogie, then

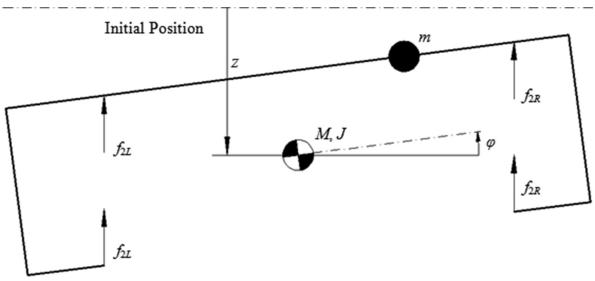

Fig. 8. Robot model under vertical force

Equation of vertical motion for robot can be written as

$$(M+m)\ddot{z} = 2f_{2L} + 2f_{2R} + (M+m)g \tag{6}$$

Where f_{2L} and f_{2R} are the vertical equivalent spring-damper force carried by bogie, and

$$\begin{cases} f_{2L} = -2k_2(z + b\phi) - 2c_2\left(\dot{z} + b\dot{\phi}\right) \\ f_{2R} = -2k_2(z - b\phi) - 2c_2\left(\dot{z} - b\dot{\phi}\right) \end{cases} \tag{7}$$

Then Eq. (6) can be written as

$$(M+m)\ddot{z}+8c_2\dot{z}+8k_2z=(M+m)g \tag{8}$$

The general solution is given by the equation

$$z(t)=A_1e^{s_1t}+A_2e^{s_2t}+\frac{(M+m)g}{8k_2} \tag{9}$$

Where A_1 and A_2 are the coefficients to be determined, and

$$s_{1,2}=-\frac{8c_2}{2(M+m)}\pm\sqrt{\left(\frac{8c_2}{2(M+m)}\right)^2-\frac{8k_2}{M+m}}.$$

Equation of rotation for robot can be written as

$$J\ddot{\phi}=2f_{2L}b-2f_{2R}b-mg(y_m-y) \tag{10}$$

Substituting Eqs. (1) and (7) into Eq. (11), then

$$J\ddot{\phi}+8c_2b\dot{\phi}+8k_2b^2\phi=-mgS(t) \tag{11}$$

The response can be written as

$$\phi(t)=\frac{1}{J\omega_{d2}}\int_0^t(-mS(t))e^{-\zeta_2\omega_{n2}(t-\tau)}\sin\omega_{d2}(t-\tau)d\tau \tag{12}$$

Where $\omega_{n2}=\sqrt{\frac{8k_2b^2}{J}}$, $\zeta_2=\frac{8c_2b}{2J\omega_{n2}}$ and $\omega_{d2}=\sqrt{1-\zeta_2^2}\omega_{n2}$.

3.3 Position and Gesture Modeling for End-Effector

Position and gesture of bogie will affect these of end-effector. Based on the proposed model above, the position and gesture of end-effector can be expressed as

$$\begin{bmatrix}y_m\\z_m\\\phi_m\end{bmatrix}=\begin{bmatrix}1&&\\&1&-S(t)\\&&1\end{bmatrix}\begin{bmatrix}y\\z\\\phi\end{bmatrix}+\begin{bmatrix}S(t)\\0\\0\end{bmatrix} \tag{13}$$

For the end-effector, horizontal displacement y_m, vertical displacement z_m and yaw angle φ_m are the corresponding position and gesture of it within motion range, which can be determined in Eq. (13) by substituting the initial conditions and prosperities.

4 Simulation

4.1 Input of End-Effector's Motion

Relative displacement of end-effector to bogie is the main factor of translation and motion of bogie. The end-effector reciprocates on the linear guide located on the bogie and process of one motion trip is divided into three stages: accelerated motion, uniform motion and decelerated motion, which can be described via a piecewise function. So the mathematic function of one motion trip can be expressed as

$$S(t) = \begin{cases} -b + \frac{1}{2}at^2 & t_1 \le t < t_2 \\ v(t-6) & t_2 \le t < t_3 \\ b - \frac{1}{2}a(t-12)^2 & t_3 \le t \le t_4 \end{cases} \tag{14}$$

Where a is relative acceleration of end-effector to bogie and a = 0.1 m/s^2, v is relative velocity of end-effector to bogie and v = 0.1 m/s, b is one-second of length of linear guide and b = 0.55 m. t_1, t_2, t_3 and t_4 are chosen to be 0 s, 1 s, 11 s and 12 s. The curve of function is plotted as shown in Fig. 9.

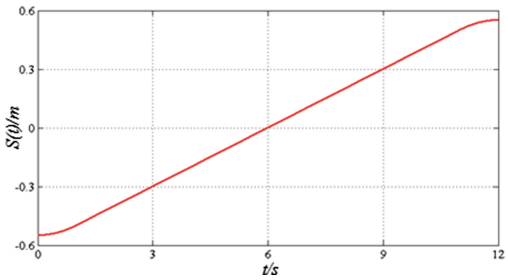

Fig. 9. Input of end-effector's motion

4.2 Simulink Model

Simulink in MATLAB is usually applied in the dynamics modeling and simulation. Based on Eqs. (4), (8) and (11), the simulation model is established in the Simulink. The simulation parameters: M = 75 kg, J = 100 kg·m^2, m = 25 kg, k_1 = 1200 N/m, c_1 = 200 Ns/m, k_2 = 3000 N/m, c_2 = 300 Ns/m. The duration of simulation is 12 s, position and gesture of bogie and end-effector, are determined with ODE 45 algorithm and curves of simulation are plotted, as shown in Fig. 10.

Under the defined working function of end-effector, the simulation results show that small change of Y displacement of bogie takes place when end-effector accelerates and decelerates. The change of Z displacement of bogie is unrelated to the motion of end-effector. Yaw angle of end-effector varies with rotation of bogie and the maximum of angel appears when end-effector locates on both ends of the linear guide of bogie. The corresponding position and gesture of end-effector is related to its working position.

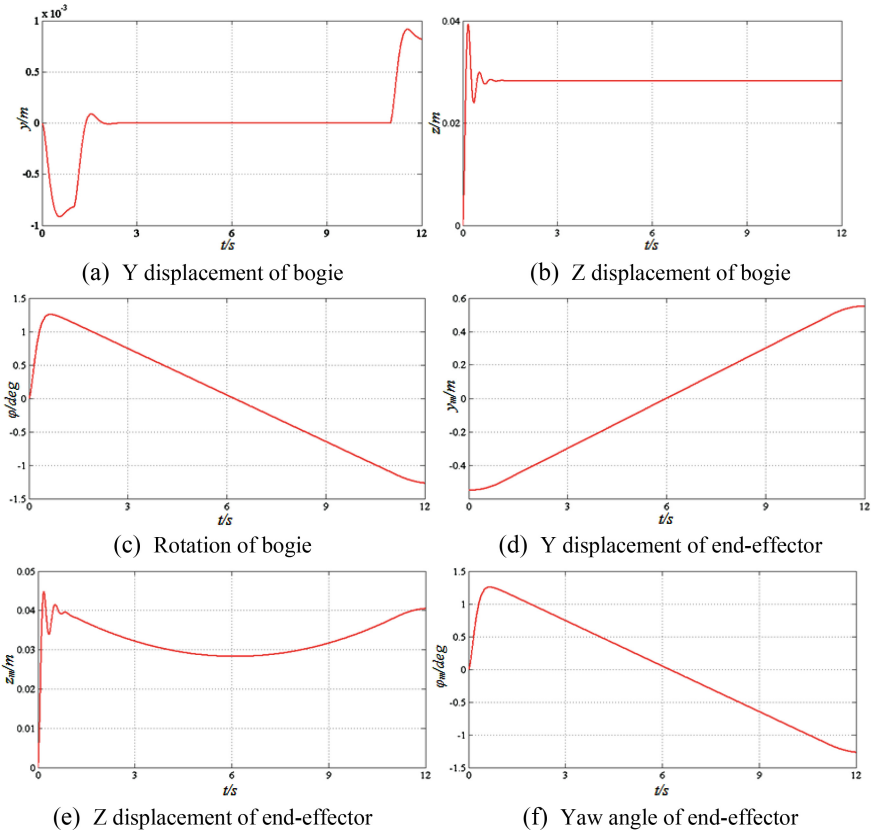

(a) Y displacement of bogie (b) Z displacement of bogie

(c) Rotation of bogie (d) Y displacement of end-effector

(e) Z displacement of end-effector (f) Yaw angle of end-effector

Fig. 10. Curves of simulation in MATLAB/Simulink

5 Experiment

A prototype of cleaning robot for solar panel is built based on the structural parameters, as is shown in Fig. 11(a), and details of the group of wheels can be seen in Fig. 11(b). After debugging PLC control system based on the working function of end-effector above, the prototype of cleaning robot can stride over the interval between panel supports without interference and end-effector washes up the surface of solar panels automatically according to the design requirements.

To test operation parameters of the prototype of cleaning robot and compare with the theory value to make further analysis, the Leica laser tracker is used to measure the yaw angle of end-effector, as is shown in Fig. 12. In addition, the reflector, as is show in Fig. 13, is the "probe" of the tracker. In the course of the experiment, the reflector is put on three different points of bogie, respectively. The coordinates of them are measured followed. Then the plane of bogie, when the end-effector moves on the linear guide of it, can be determined by the following equation:

$$\begin{vmatrix} y_2 - y_1 & y_3 - y_1 \\ z_2 - z_1 & z_3 - z_1 \end{vmatrix} \cdot (x - x_1) + \begin{vmatrix} z_2 - z_1 & z_3 - z_1 \\ x_2 - x_1 & x_3 - x_1 \end{vmatrix} \cdot (y - y_1) + \begin{vmatrix} x_2 - x_1 & x_3 - x_1 \\ y_2 - y_1 & y_3 - y_1 \end{vmatrix} \cdot (z - z_1) = 0 \tag{15}$$

Where (x_1, y_1, z_1), (x_2, y_2, z_2) and (x_3, y_3, z_3) are the coordinates of these three different points.

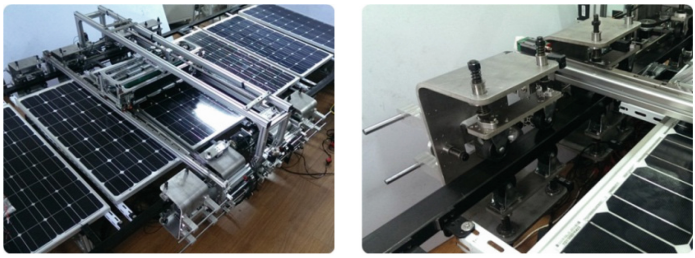

(a) Robot in working condition (b) Close-up of the group of wheels

Fig. 11. Prototype of cleaning robot

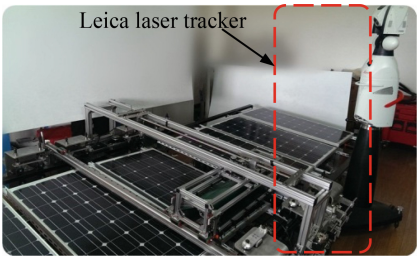

Fig. 12. Robot measurement system in working condition

Fig. 13. Close-up of the group of wheels

The three planes of bogie when end-effector is on the beginning position, the middle position and the end position of linear guide are measured. The measurement data is shown in Table 1. The rotation angle of bogie can be calculated as follows

$$\theta = \arccos\left(\frac{|A_iA_j + B_iB_j + C_iC_j|}{\sqrt{A_i^2 + B_i^2 + C_i^2} \cdot \sqrt{A_j^2 + B_j^2 + C_j^2}}\right), 0^\circ \le \theta \le 180^\circ \tag{16}$$

Where (A_i, B_i, C_i) and (A_j, B_j, C_j) are the normal vectors of the plane π_i and π_j, which are determined by Eq. (16). Moreover, this angle is also the yaw angle of end-effector according to analysis in Part 3.

Table 1. Experimental data

Position	Point	x/mm	y/mm	z/mm
Beginning	1st	2629.49	1652.31	−565.69
	2nd	2414.81	1698.09	−563.50
	3rd	2161.88	480.73	−660.74
Middle	1st	2629.96	1653.76	−569.12
	2nd	2415.01	1699.58	−566.90
	3rd	2164.62	484.25	−658.84
End	1st	2630.78	1654.59	−571.56
	2nd	2417.63	1699.91	−569.42
	3rd	2165.17	486.25	−657.59

After substituting these data above into Eqs. (15) and (16), the yaw angles of end-effector on the beginning position and the end position are 0.17° and 0.24°, respectively, which are smaller than the results obtained in Part 4. The reason for this situation is that the springs which have bigger stiffness coefficients are assembled to prevent the bogie from turning out of metal rails of panel support. The yaw angle of end-effector becomes smaller, consequently. Through experiments with a series of springs, the stiffness and damping coefficients of springs affect the position and gesture of end-effector. Intuitively, the conclusion that gesture of end-effector changes as its working position changes can be obtained.

6 Conclusions

(1) As the solution to automatic cleaning of solar panel, a cleaning robot based on monorail bogie is described and its operational principle is presented.
(2) Five hypotheses are proposed based on the mechanical structure and working condition of bogie, then the robot-rails system is simplified as a double masses-spring-damper model and equations of motion for cleaning robot are established.
(3) The general solutions of differential equations of motion for robot are given, position and gesture of end-effector are determined.
(4) The simulation model under the defined working function of end-effector is built using Simulink. The results show that motion of end-effector has a minimal effect on the position of bogie and the position and gesture of end-effector are related to its working position.
(5) A prototype is fabricated, and then tested using the Leica laser tracker. As a consequence, the results of experiment have proved that the design of this cleaning robot and the analysis model are correct and practical.

Acknowledgements. The authors would like to acknowledge the financial support of the Natural Science Foundation of China under Grant 51475050, Shanghai Science and Technology Committee under Grant 12510501100, the Natural Science Foundation of Shanghai City under Grant 14ZR1422700, and the Technological Innovation Project of Shanghai University of Engineering Science under Grant E1-0903-15-01012.

References

1. Chen, F., Wang, L.: On distribution and determinants of PV solar energy industry in China. Resour. Sci. **34**(2), 287–294 (2012)
2. Mastromauro, R.A., Liserre, M., Dell'Aquila, A.: Control issues in single-stage photovoltaic systems: MPPT, current and voltage control. IEEE Trans. Ind. Inform. **8**(2), 241–254 (2012)
3. Lu, L., Xu, T., Chen, W., et al.: The role of N-doped multiwall carbon nanotubes in achieving highly efficient polymer bulk heterojunction solar cells. Nano Lett. **13**, 2365–2369 (2013)
4. Guangshuang, M., Dedong, G., Shan, W., et al.: Mechanics modeling of dust particle on solar panel surface in desert environment. Trans. Chin. Soc. Agric. Eng. **30**(16), 221–229 (2014)
5. Schraft, R.D., Wanne, M.C.: The aircraft cleaning robot "SKYWASH". Ind. Robot **20**(6), 21–24 (1993)
6. Zhu, J., Sun, D., Tso, S.K.: Development of a tracked climbing robot. J. Intell. Robot. Syst. **35**(4), 427–443 (2002)
7. Bräuning, U., Orlowski, T., Hornemann, M.: Automated cleaning of windows on standard facades. Autom. Constr. **9**(5–6), 489–501 (2000)
8. Shixue, G.: Design and Optimization of the Manipulator Parts of Cleaning Machine of Solar Panel. Lanzhou University of Technology (2014)
9. The homepage of Ecoppia Empowering Solar. http://www.ecoppia.com/ecoppia-e4
10. Liqun, P.E.N.G., Dawen, L.I.N., Xinglei, W.U., et al.: Experimental design and research of straddle-type monorail vehicle bogie traction mechanism. Railw. Locomotive Car **34**(2), 70–73 (2014)
11. Ivanchenko, I.: Substructure method in high-speed monorail dynamic problems. Mech. Solids **43**(6), 925–938 (2008)
12. Bruni, S., Goodall, R., Mei, T.X., et al.: Control and monitoring for railway vehicle dynamics. Veh. Syst. Dyn. **45**(7), 743–779 (2007)
13. Wanming, Z.: Vehicle-Track Coupling Dynamics, 3rd edn. Science Press, Beijing (2007)
14. Alkan, V., Karamihas, S.M., Anlas, G.: Experimental analysis of tire-enveloping characteristics at low speed. Veh. Syst. Dyn. **47**(5), 575–587 (2009)
15. Jun, Ma., Kun, Y.: Modeling simulation and analysis of radial spring tire model. Agric. Equip. Veh. Eng. **52**(12), 33–37 (2014)
16. Meirovitch, L.: Fundamentals of Vibrations. The McGraw-Hill Companies Inc., New York (2001)